

Apricot pomaces extract (*Prunus Armeniaca L.*) as a highly efficient sustainable corrosion inhibitor for mild steel in sodium chloride solution

V.I. Vorobyova,¹ M.I. Skiba² and I.M. Trus²

¹National Technical University of Ukraine “Igor Sikorsky Kyiv Polytechnic Institute”,
Kyiv, Ukraine. Ave Peremogy 37, Kiev, 03056, Ukraine

²Ukrainian State Chemical-Engineering University, Gagarin Ave. 8, Dnipro, 49005,
Ukraine

*E-mail: vorobyovavika1988@gmail.com

Abstract

The present study was carried out to identify the components present in the ethanol apricot pomace extract by GC-MS analysis. Various experimental models including iron(III) reducing capacity, total antioxidant capacity, DPPH radical scavenging activity were used for characterization of antioxidant activity of the extract. Weight loss investigation, potentiodynamic polarization, and FTIR techniques were used to study the corrosion inhibition. The maximum inhibition efficiency of 94.6% was achieved by using 500 ppm of the inhibitor. Scanning electron microscopy (SEM) and atomic force microscopy (AFM) analysis were used to characterize the protective film. AFM also illustrated an improvement in the surface properties of the samples in the presence of APE. The influence of the immersion period on inhibition efficiency was evaluated. The GC-MS experimental results show that the major compounds of the APE are 3,4,5-trihydroxybenzoic acid, chlorogenic acid, 3-(3,4-dihydroxyphenyl)-2-propenoic acid, 2-(3,4-dihydroxyphenyl)-3,5,7-trihydroxy-4*H*-chromen-4-one, and catechin. The results revealed that in the attendance of the APE and with the immersion time progress up to 48 h, the inhibition capacity of inhibitor was promoted. The mechanism of action of the inhibitor is also discussed. Quantum chemical parameters calculated for the molecules contained in the aqueous extract are interpreted to predict the corrosion inhibition efficiency of the considered extract. The theoretical study gave insights to the active sites, chemical reactivity and possible interaction mechanism between the inhibitor compounds and mild steel surface. The apricot pomace extract studied in this work are potential multifunctional inhibition materials as they showed good antioxidant and anticorrosion properties.

Keywords: green corrosion inhibitors, antioxidant/free radical scavenging activity, phytochemicals, metals and alloys.

Introduction

Nowadays, mild steel is known as the most famous alloy in a wide range of industrial applications such as metal processing, equipment, and construction [1–6]. Corrosion inhibitors are commonly used in industry to reduce the corrosion rate of metals and alloys. For mild steel protection in chloride-containing media, a large number of inorganic and organic corrosion inhibitors have been studied. The use of traditional corrosion inhibitors is now limited because of an increasing concept of “green chemistry” in the field of science, technology, and engineering [1–6]. This has prompted researchers to find out some cheap and effective “green” inhibitors [1, 7–11]. Consequently, organic molecules extracted from food by-products appear as an alternative in the field of corrosion inhibition due to their biodegradability and easy availability. In this regard, the highly effective environmental friendly corrosion inhibitors obtained from natural products such as different parts of plants like root, seeds, leaves, stem, flower, and fruits are recently attracted the high consideration of the researchers. However, the inhibitor extracted from a waste without harm to plants and environment was seldom reported. Actually, in the present ecological context, plants, food, forest or agro-industrial wastes extracts appear as an alternative to fulfil the conditions of REACH regulation and European directives on the wastewater reject. The inhibition ability of the plant and agro-food wastes extracts is generally attributed to the presence of naturally phytochemical compounds which have antioxidant properties. It has also been found that plant components (biopolymers, proteins, flavonoids, and alkaloids) exhibit effective inhibitory activity based on their antioxidant activity derived from their structure. Importantly, the correlation between antioxidant/free radical scavenging activity of the extracts and the inhibition action was observed [12]. However, due to the large variety of molecules contained in natural extracts, the inhibition mechanisms remain largely unknown. So, it is an interesting and useful task to find new sources for highlighting anticorrosive and antioxidant active compounds and to obtain organic compounds for their further use as inhibitors of corrosion in the corrosive media. Apricot fruits (*Prunus Armeniaca L.*) are valued and highly consumed all over the world, both for their flavor and for nutritional qualities. Ukraine is one of the major apricot producers in the world with the approximate annual yield of 160 000 tonnes/year of fresh fruit, seeds, and kernels, respectively.

Actually, apricot cake remaining after pressing of the fruit constitutes almost 60% of the total fruit mass [18]. The successful utilization of this natural waste may also provide an option for resource recovery. This waste is valuable since it is a rich source of the functional compound and can be used for corrosion inhibition of steel. In the literature, one can also find no information about possible applications of the apricot cakes and its extracted compounds for the development of corrosion inhibitor of mild steel in neutral media. The corrosion protection of mild steel in 1 M H_3PO_4 solution by apricot juice was studied only in one paper [13].

The aim of the present work firstly is to determine the chemical composition and antioxidant activities of apricot pomace extract (APE). Secondly, is to evaluate the corrosion inhibition effect of APE as “green” corrosion inhibitor of mild steel in neutral media and also investigate the constituents that provide inhibitive action of the extract.

1. Materials and methods

The apricot (*Prunus Armeniaca L.*) cultivar known under local name “Favorite” were harvested (during July 2019) in two geographical regions of Ukraine (Kherson, Nikolaev). The apricot pomace was supplied by an agro-food company (Vinni Frut) located in the city of Vinnytsia, Ukraine.

The mild strips were purchased from Rocholl, Aglasterhausen, Germany. Corrosion test samples (electrodes) were manufactured from mild steel St3 (European analog Fe37-3FN). The composition (wt. %) of mild steel samples used in this study was as follows: (93.9% Fe, 1.2% P, 1.1% Mn, 1.0% Si, 0.7% Cr and 1.7% Ni).

Analytical grade ethanol (EtOH) and other chemicals were obtained from the general suppliers. All reagents were of analytical grade and were purchased from Sigma-Aldrich (Milan, Italy).

1.1 Preparation of extract

The apricot press pomace was obtained by cold pressing. The cake is made of pressed skins and pulp residues (of fresh apricots). The apricot press pomace extract was obtained with ethanol (EtOH) in a Soxhlet apparatus. The Soxhlet extraction was performed in the optimum condition. 5.0 g of ground material was extracted with 150 mL 95% ethanol in a Soxhlet apparatus for 2 h. The solvent was removed at 40°C in a rotary vacuum evaporator under a nitrogen stream. 1 g of dry extract was dissolved in 100 mL ethanol to give a stock solution of 1% (w/v) inhibitor. Then, appropriate volumes of 1% APE solution were added into the blank corrosive electrolyte (0.5 M NaCl) in order to obtain electrolytes containing different concentrations of APE in the range of 50–500 ppm.

2.2 Identification of chemical profile

2.2.1 Gas chromatography–mass spectrometry (GC–MS)

GC-MS analyses were carried out on a Varian 450-GC coupled to a Varian 220-MS IT (Agilent Technologies) through an electron impact (EI) ion source. A 5%-phenyl-methyl polysiloxane (HP5MS) capillary column (30 m×0.25 mm i.d., 0.25 μm) (Agilent Technologies) was used to separate the analytes, with He as a carrier gas at a flow rate of 1 mL/min. Oven temperature was initially kept at 140°C for 5 min, ramped at 4°C/min to 310°C and held for 2.5 min. A sample volume of 1 μL was injected at a split ratio of 1:25. Injector and transfer line temperatures were 240°C and 290°C, respectively. Spectra were recorded in full scan (from 50 to 600 m/z), with the EI source operating at a potential of 70 eV in positive ion mode, and a source temperature of 200°C. Instrument control and

data processing for GC-MS analyses were done with MS Workstation v6.9.3 (Agilent Technologies) [19]. The components were identified by comparing the peak retention time in the chromatogram and the complete mass-spectra of individual components with the corresponding results for pure compounds in the NIST-5 Mass Spectral Library [20]. The relative contents of the chemical components of the extract were found with the help of the method of internal normalization of the areas of peaks without correcting the sensitivity coefficients.

2.2.2 Fourier transformation infrared spectroscopic studies (FTIR)

For a better understanding of inhibition mechanism, the apricot cake extract was characterized through Fourier transform infrared spectroscopy (FTIR) in attenuated total reflection mode (Pike Technologies, GladiATR for FTIR with diamond crystal) in the range of 4000–400 cm^{-1} .

2.3 Antioxidant assays

2.3.1 Determination of total antioxidant capacity by phosphomolybdenum method

The total antioxidant capacity of the extracts different solvents were evaluated by the phosphomolybdenum method as described by the method of Prieto *et al.* (1999) [21]. The analysis is based on the reduction of Mo(VI) to Mo(V) with an extract and, as a consequence, the formation of a green phosphate/Mo(V) complex at acidic pH. The volume of the extract to the reagent was 1:10, 0.5 mL of each sample solution and ascorbic acid (100 $\mu\text{g}/\text{mL}$) were taken for the experiment with 5 mL of reagent (0.6 M sulfuric acid, 28 mM sodium phosphate and 4 mM ammonium molybdate). The blank solution contained 5 mL of the reagent solution and the corresponding volume of the solvent used, which was used for the sample. All tubes were closed and incubated in a boiling water bath at 95°C for 90 minutes. After the samples had been cooled to room temperature, the absorbance of the solution of each sample was measured at 695 nm against the blank using a UV–Vis spectrophotometer (UV-5800PC spectrophotometer, FRU, China).

2.3.2 Determination of antioxidant activity in terms of reducing power

Fe(III) reduction is often used as an indicator of electron donating activity, which is an important indicator of the phenolic antioxidant effect [17]. Extracts, which have reduction potential, react with potassium ferricyanide (Fe^{3+}) to form potassium ferrocyanide (Fe^{2+}), which then reacts with ferric chloride to form a ferric ferrous complex that has an absorption maximum at 700 nm. To prepare the reaction solution, a different amount of the extract, after the rotary evaporator, was mixed (0.005 g, 0.01 g, 0.015 g, 0.02 g, 0.025 g) was dissolved in an appropriate solvent (1 mL) and 1 mL phosphate buffer (0.2 M, pH 6.6) and 1 mL of potassium ferricyanide solution (1%). The resulting solution was incubated at 50°C for 20 minutes. Then 1 mL of trichloroacetic acid (10%) was added to terminate the reaction and was quenched under running water for 5 minutes, the resulting mixture was

centrifuged at 3000 rpm for 10 minutes. An aliquot of 2 ml was then removed from the top layer of each solution, to which were added 2 mL of distilled water and 0.4 mL of ferric chloride solution (0.1%). The solution absorbance was measured at 700 nm. Increasing absorbance of the reaction mixture indicates increasing reducing power. Results were expressed as a mean \pm standard deviation (SD) of 5 replicate measurements, with ascorbic acid and butylated hydroxytoluene (BHT) as a reference reducing agent.

2.3.3 DPPH radical scavenging activity

The method is based on the purification of DPPH by adding radical particles or an antioxidant that discolor the DPPH solution [17]. The degree of colour change is proportional to the concentration and efficiency of the antioxidants. Antioxidant activity is then measured by the decrease in absorption at 517 nm. Dry extract (RE) was dissolved in ethanol at various concentrations ranging from 0.01 to 0.5 mg/ml. Each dilution (0.5 ml) was mixed with 3 ml of an ethanolic solution of DPPH (0.1 mmol). The mixture was incubated in the dark at room temperature and the absorbance of the DPPH solution was measured at $\lambda = 517$ nm (Jasco V-530, Japan) to and 30 minutes after adding the extract (sample). In the blank, ethanol was used in place of the sample. Ascorbic acid and gallic acid, BHT were used as a positive control.

2.4 Surface morphology studies (SEM & AFM analysis)

The AFM analysis was performed in tapping mode using AFM (Dimension Icon ScanAsyst) supported by NanoScope V having spring constant of 42 N/m and tip radius 10 nm. The measurements were done at room temperature and a scan rate of 0.4 Hz over an area of $50 \times 50 \mu\text{m}^2$ [22]. The morphologies of mild steel surfaces after 20 days of immersion in chloride solution (0.5 M NaCl solution) without and with the presence of plants extract were examined by scanning electron microscope. The surface morphology and coating were examined by FEI E-SEM XL 30 (Detection of secondary electrons). For SEM images, 1 cm^2 sample was taken.

2.5 Weight loss measurements

For weight loss estimations the mild steel specimens were set up as ASTM G 31-72 [23]. Mild steel coupons of dimensions $5.0 \times 3.0 \times 0.2$ cm were used in the weight loss experiments. Before each experiment, the coupons were abraded and polished using emery papers (grades 220–1200), washed thoroughly with distilled water, degreased with acetone and finally dried. The initial weight of each coupon was taken (before immersion) using an analytical balance. Then, the specimens were immersed in 0.5 M NaCl solution without and with different concentrations of the apricot pomace extract. After the immersion period, the specimens were taken out, washed, dried and weighed again. The difference in weight was calculated from the initial and final weight of the specimens. All the experiments were performed in triplicate and the average weight loss values were recorded.

Three values were obtained by repeating experiments three times, and an average value was recorded. Average values of the weight loss data were used in corresponding calculations.

2.6 Electrochemical measurements

Electrochemical experiments were carried out in the conventional three-electrode cell with a platinum counter electrode (CE), a saturated calomel electrode (SCE) coupled to a fine Luggin capillary as the reference electrode (RE) and a working electrode (WE). The carbon steel working electrode was designed with a fixed exposed surface area of 0.385 cm^2 . For the electrochemical experiments, the surface area of the platinum counter electrode is larger than that of WE, and the CE is counter to the total exposed surface of WE. Thus, the electrical field distribution could be uniform. All electrochemical measurements were carried out using a PARSTAT 2273 advanced electrochemical system (Princeton Applied Research). In order to minimize ohmic contribution, the tip of the Luggin capillary was kept close to WE. Experiments were carried out in duplicate to ensure reproducibility of results. At the beginning of the tests, the working electrode was immersed in the test solution for 1 h to get a stabilized open circuit potential.

The linear polarization technique (LPR) was applied to study time variation of the corrosion rate [24, 25]. Polarization resistance values R_p for each probe were measured automatically every 15 min in a galvanostatic mode. R_p was determined as a quotient of the potential response to the applied current. The density of polarizing current was $i = 5 \text{ } \mu\text{A}/\text{cm}^2$. The conventional B value of 26.1 mV was used to obtain the corrosion rate (mm/y) from measured R_p values. This B value is commonly used in neutral water solutions. Data for three probes were averaged.

2.7 Quantum chemical studies

Optimization of molecular structure was performed by using the HyperChem 8.0 programming. At the preliminary stage of calculations, the geometries of parent molecules in the gas phase have been first optimized using the semi-empirical PM3 method implemented in the HyperChem 8 program package. Next, the energy of the obtained conformers was minimized using the MM+ force field and PM3 parameterizations within the restricted Hartree-Fock (RHF) formalism. The optimized structures which had the minimum energy values were selected for further calculations. Key parameters, for example, the energy of LUMO (E_{LUMO}), HOMO (E_{HOMO}), the energy gap (ΔE) between LUMO and HOMO, electronegativity (χ), softness (σ) and the hardness (η) of the molecules were taken from those optimized structures in a gas phase. It has been suggested that the theoretical calculations the gas phase are a useful method because the results obtained in the gas phase show no significant variation from those obtained in aqueous phase [26–31].

3. Results and discussion

The results of phytochemical analysis of the EtOH apricot pomace extract are given in Table 1 (see Table 1) and the GC-MS spectrum is shown in Figure 1. As a result of the GC-MS analysis, 41 phytochemical compounds were identified in the apricot pomace extract [32]. This result indicates that APE contains different classes of organic substances in their composition, which can act as corrosion inhibitors. The maximum amount of the component present in APE are: 3,4,5-trihydroxybenzoic acid (Gallic acid) (4.19 percent), chlorogenic acid (3.82 percent), 3-(3,4-dihydroxyphenyl)-2-propenoic acid (caffeic acid) (2.71 percent), 2-(3,4-dihydroxyphenyl)-3,5,7-trihydroxy-4*H*-chromen-4-one (quercetin) (7.1 percent), catechin (2.94 percent).

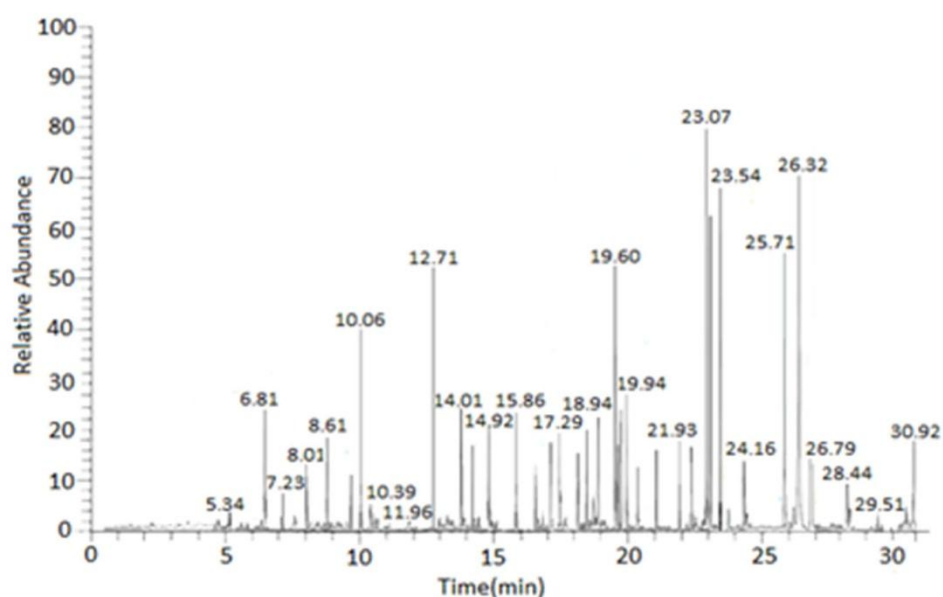


Figure 1. GC-MS spectral chromatogram of apricot pomace extract (APE).

According to the chromatogram, five aldehydes are identified by GC-MS in the APE, namely, hexanal (1.28 percent), benzaldehyde (3.18 percent), heptanal (0.64 percent), 2,6,6-trimethylcyclohexene-1-carbaldehyde (β -cyclocitral) (3.24 percent), 2-phenylacetaldehyde (1.73 percent), terpene alcohols (27.8 percent) and saturated and unsaturated fatty acids (18.91 percent) represented by (9*Z*,12*Z*)-octadeca-9,12-dienoic acid (linoleic acid), hexadecanoic acid, 1-tetradecanoic acid, octadecanoic acid. All individual chemical compounds are known as inhibitors for several metals [33, 34]. The effect of 2-phenylacetaldehyde and hexanal on the corrosion behavior of steel was studied [35] through weight loss, electrochemical, SEM, AFM, quantum chemical calculation methods. It was found that the inhibition effect of 2-phenylacetaldehyde was associated with layer-by-layer mechanism formation of a protective film. Interestingly, the electrochemical and spectroscopic studies have revealed that unsaturated aldehydes (2-phenylacetaldehyde) and

phenolic compounds (thymol and carvacrol) can polymerize on metallic surfaces and show excellent corrosion protection [33–35].

Table 1. GC-MS analysis result of APE.

Holding time <i>t</i> , min	Name of the compound	Weight ratio, (%)
5.34	(<i>Z</i>)-3-Hexenol	0.8
6.81	3,4,5-Trihydroxybenzoic acid (gallic acid)	4.19
7.23	2-Hexanone	1.05
7.69	Mannose	0.24
8.01	3-Hexanone	1.72
9.58	Hexanal	1.28
10.06	Benzaldehyde	3.18
11.96	Heptanal	0.64
12.71	Phenylacetaldehyde	1.73
14.01	(<i>E</i>)-2-Hexenyl acetate	1.06
14.12	(1 <i>S</i> ,3 <i>R</i> ,4 <i>R</i> ,5 <i>R</i>)-3-[[(<i>2E</i>)-3-(3,4-Dihydroxyphenyl)prop-2-enoyl]oxy]-1,4,5-trihydroxycyclohexanecarboxylic acid (chlorogenic acid)	3.82
14.37	5-Butyloxolan-2-one (γ -octalactone)	0.71
14.43	<i>endo</i> -1,7,7-Trimethyl-bicyclo[2.2.1]heptan-2-ol (isoborneol)	0.43
14.58	5-Methyl-2-(propan-2-yl)phenol (thymol)	3.56
14.92	2,6,6-Trimethylcyclohexene-1-carbaldehyde (β -cyclocitral)	3.24
15.74	3-(3,4-Dihydroxyphenyl)-2-propenoic acid (caffeic acid)	2.71
15.86	(<i>Z</i>)-3,7-Dimethyl-2,6-octadien-1-ol (nerol)	3.09
16.74	(9 <i>Z</i> ,12 <i>Z</i> ,15 <i>Z</i>)-9,12,15-Octadecatrienoic acid (α -linolenic acid)	1.94
16.98	(2 <i>R</i> ,3 <i>S</i> ,4 <i>R</i> ,5 <i>R</i>)-2,3,4,5,6-Pentahydroxyhexanal (<i>D</i> -glucose)	0.98
17.06	(<i>2E</i>)-3,7-Dimethyl-2,6-octadien-1-ol (geraniol)	3.49
17.29	(9 <i>Z</i> ,12 <i>Z</i>)-Octadeca-9,12-dienoic acid (linoleic acid)	3.29
18.24	Hexadecanoic acid (palmitic acid)	2.61
18.32	3,7-Dimethylocta-1,6-dien-3-ol (linalool)	3.32
18.94	1-Tetradecanoic acid	3.29

Holding time <i>t</i> , min	Name of the compound	Weight ratio, (%)
19.60	Octadecanoic acid (stearic acid)	5.71
19.62	(9 <i>Z</i>)-Octadec-9-enoic acid	4.01
20.67	(7 <i>aR</i>)-5,6,7,7 <i>a</i> -Tetrahydro-4,4,7 <i>a</i> -trimethyl-2(4 <i>H</i>)-benzofuranone	2.04
21.09	(<i>Z</i>)-3-Hexenyl butanoate	2.91
22.18	(1 <i>R</i> ,2 <i>S</i> ,6 <i>S</i> ,7 <i>S</i> ,8 <i>S</i>)-8-Isopropyl-1,3-dimethyltricyclo[4.4.0.0]dec-3-ene	3.09
23.07	2-(3,4-Dihydroxyphenyl)-3,5,7-trihydroxy-4 <i>H</i> -chromen-4-one (quercetin)	7.1
23.08	3-Cyclohexen-1-ol, 4-methyl-1-(1-methylethyl) (4-terpineol)	6.24
23.54	2-(4-Methylcyclohex-3-en-1-yl)propan-2-ol (α -terpineol)	6.61
23.82	(3 <i>E</i>)-4-(2,6,6-Trimethylcyclohex-1-en-1-yl)but-3-en-2-one (β -ionone)	0.47
24.16	(2 <i>R</i> ,3 <i>S</i>)-2-(3,4-Dihydroxyphenyl)-3,4-dihydro-2 <i>H</i> -chromene-3,5,7-triol (catechin)	2.94
24.48	(2 <i>E</i>)-3-(4-Hydroxyphenyl)prop-2-enoic acid (<i>p</i> -coumaric acid)	1.94
26.32	Dihydro-5-octyl-2(3 <i>H</i>)-furanone	0.65
26.79	3,7,11-Trimethyl-1,6,10-dodecatrien-3-ol (nerolidol)	2.52
28.44	3,3',4',5,7-Pentahydroxyflavone (isoquercetin)	1.74
29.51	Stigmasterol	0.43
30.08	Eicosanic acid	0.39
30.92	β -Sitosterol	2.13

The antioxidant activity of the extract was analyzed in several methods because the evaluation of antioxidant properties of plants cannot be carried out accurately by a single universal method. In this study, the antioxidant activity of the ethanol extract was evaluated using 3 different assays.

The total antioxidant activity was measured by phosphomolybdate method. Also, it is a quantitative one, since the antioxidant activity is expressed as the number of the equivalent of ascorbic acid (mg/g plant extract). Extract of cake apricot exhibited concentration-dependent antioxidant capacity with respect to ascorbic acid equivalents (see Table 2). The total antioxidant activity is 460.86 ± 2.63 mg of AsA/g of the extract.

Table 2. Characterization of antioxidant activity of the apricot pomace extract.

Total antioxidant capacity (mg ASE/g of the extract)	Reducing power, mg of ASE/g of the extract				
	Concentration, mg/ml				
460.86±2.63	0.5	1.0	1.5	2.0	2.5
	3.3152	3.3152	3.3152	3.3152	3.341

This potent antioxidant activity may be attributed to its high phenolic and flavonoid contents. The total antioxidant activity of apricot pomace extract is the result of individual activities of each of the antioxidant compounds present such as tocopherols, carotenoids, and phenolic compounds, the latter being the major phytochemicals responsible for the antioxidant activity of plant materials. Even if a sample exhibits high activity with one of these methods, it does not always show similar good results with all other methods. Therefore, it is essential to evaluate samples accurately by several methods. Reducing power is associated with antioxidant activity and can serve as a significant reflection of antioxidant activity. Compounds with a reducing power show that they are electron donors that have the ability to reduce oxidized intermediates of the processes of lipid peroxidation, they can act as primary and secondary antioxidants. Higher absorbance of the reaction mixture indicates higher reductive potential. Table 2 shows the concentration–absorbance relation for the reducing powers of the extracts. The reducing power of the extracts increased with increase in their concentrations. The extracts exhibited fairly good reducing power. The apricot pomace extract radical scavenging activity was studied by DPPH method using ascorbic acid as the standard and the results are depicted in Table 3. The results indicate the efficacy of the apricot pomace extract in scavenging the DPPH radicals depending on concentration.

Table 3. DPPH radical activity of the apricot pomace extract.

Concentration, mg/ml	Percentage of inhibition (%)
0.01	33.2±1.6
0.05	46.1±1.1
0.1	56.7±0.9
0.2	68.9±0.9
0.5	92.6±0.9

The antioxidant activity of APE was high (92%) at 100 µg/mL. The radical scavenging activity of this extract is may be due to the involvement of phenolic compounds and also owing to the existence of other antioxidant secondary metabolites like flavonol, terpenoids, tannins *etc.* [17]. Thus, the analysis of the composition and evaluation

of the antioxidant properties of the apricot pomace extract indicates that it contains a wide range of organic substances and has a high antioxidant capacity, and therefore is a potential raw material for use as a corrosion inhibitor of metals. The efficiency of various concentrations of apricot pomace extract in 0.5 M NaCl medium for a period of 26 days obtained *via* weight loss method is listed in Table 4, indicating that the solution with 500 ppm possessed maximum efficiency for inhibition. The effectiveness of inhibition increased with concentration.

Table 4. Inhibition efficiency and surface coverage (gravimetric data, 624 h immersion) of mild steel in 0.5 M NaCl with the inhibitor.

The concentration of the inhibitor, ppm	Inhibition efficiency (IE), %	Surface coverage, %
0	–	–
50	25.8	0.258
100	58.9	0.589
150	68.9	0.689
200	72.5	0.725
250	74.2	0.742
300	78.9	0.789
400	80.1	0.801
500	94.6	0.946

The reason behind this fact can be given as adsorption of the organic matters of the extracts on the metal surface, which increased the surface coverage area as well as suppressed corrosion reactions rate. However, no significant corrosion inhibition was acknowledged beyond 500 concentrations of the extract, which might be resulted from saturation of inhibitor's adsorption rate on a mild steel surface.

The immersion time is an important parameter in assessing the stability of corrosion inhibitive properties of organic compounds. Figure 2 and Figure 3 illustrates the effect of immersion time on the inhibitive performance of APE. Immersion time was found to have a profound effect on the corrosion inhibition performance by the apricot pomace extract. The formation process of the protective layer can be classified into two steps, namely primary adsorption (1–30 hours) as the first step and then a slow chemical transformation (polymerization) the molecules that were adsorbed on the steel surface (40–48 hours). It is evident from Figure 2 that inhibition efficiency in 0.5 M NaCl containing APE slowly increased up to the moment when it reached 30 h of immersion, and then it rapidly increased between 40 h and 48 h of immersion till reached its saturation. According to the results above, the maximum inhibition efficiency (about 97%) was obtained at 500 ppm APE extract after 48 h immersion. This may suggest that these optimal conditions allow

the extract molecules to be adsorbed on the steel, forming a thin and uniform film. This suggested that the corrosion protectiveness of APE film-forming on the steel surface was enhanced by prolonging the APE treatment.

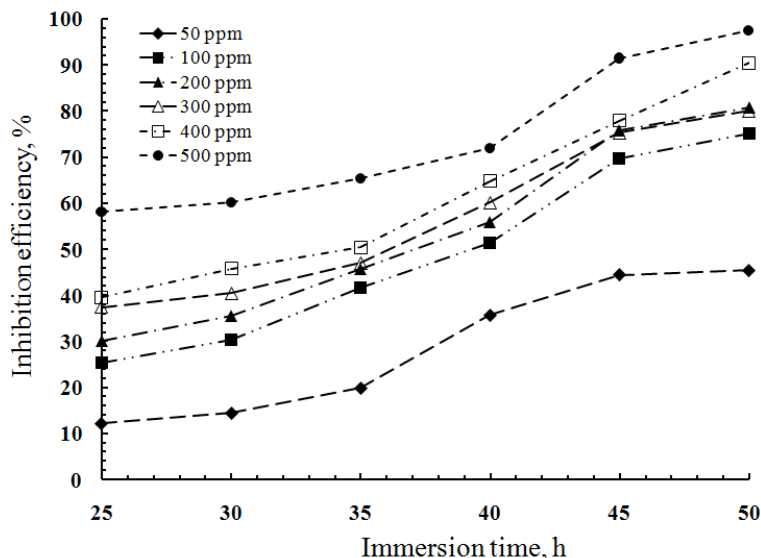


Figure 2. The relationship between inhibition efficiency and immersion time mild steel in 0.5 M NaCl solution with 50–500 ppm APE.

The effect of immersion time in a 0.5 M NaCl solution with APE on the weight loss rate indicated that APE not only keeps its inhibitive activity for steel but also improves its effectiveness over the long-term immersion due to the synergistic influence of the main compounds which offer an additional protection.

The relatively poor protection afforded by apricot pomace extract on steel at the initial immersion compared to the results obtained at longer exposure suggests that the formation of a highly protective and stable inhibitor layer on steel surface might need more time than 1–30 h to evolve completely. Similar results were obtained for steel corrosion inhibition by grape and rape pomace extracts in conditions of periodic condensation of moisture [35–41]. When the immersion time was prolonged beyond 210 h, a decrease of the stability of the protective layer was observed as result of desorption of APE molecules and/or diffusion process through the interface protective layer/electrolyte (see Figure 3).

Therefore, on the basis of the immersion time results, one can note the excellent inhibition properties of APE after 48 h of immersion in the chloride-containing medium and one can suggest that the adsorption mechanism on the carbon steel surface involves two types of interactions, chemisorption and physisorption.

The anodic and cathodic polarization behavior of various immersion times in the inhibitor was studied by the potentiodynamic polarization technique. The polarization curves are shown in Figure 4. The anodic and cathodic corrosion current density curves in presence of inhibitors are shifted towards lower current density region as compared to the

blank. This reveals that the inhibitors decrease the corrosion current and thus reduce the corrosion rate. The presence of protective film on the surface that formed in solution with apricot pomace extract result marked a shift in the cathodic branches and to a lesser extent in the anodic branches of the polarization curves. Thus the inhibitors are said to be mixed type, but predominantly cathodic. Probably, the organic moieties of apricot pomace extract adsorbed on the metal surface and increased insulating behavior of modified mild steel electrode, which caused lowering in corrosion current values.

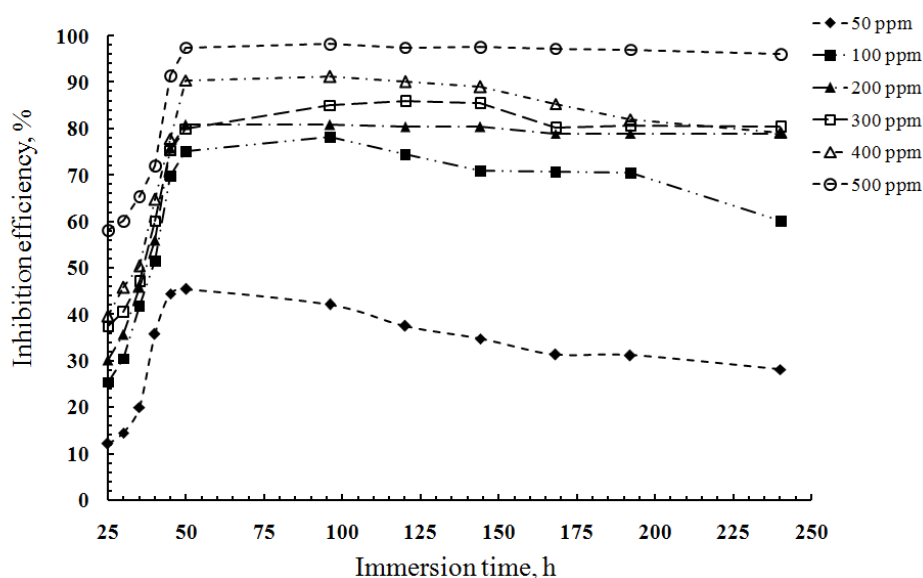


Figure 3. Effect of change in immersion time on inhibition efficiency of APE for the steel in 0.5 M NaCl solution with 50–500 ppm of APE.

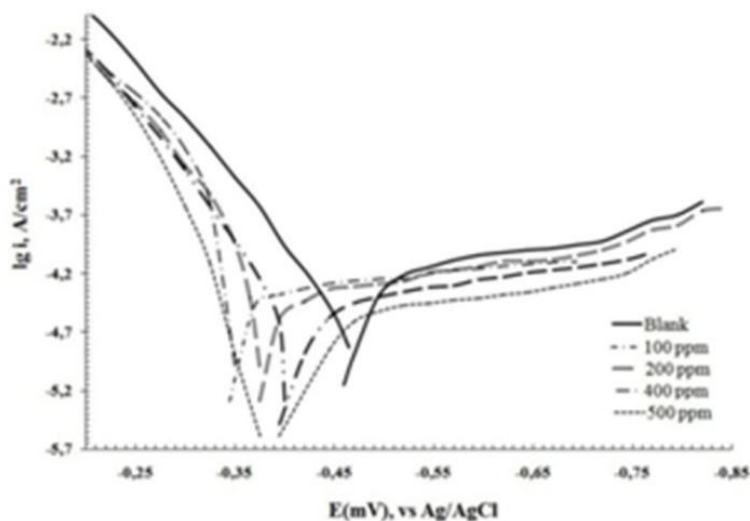


Figure 4. Potentiodynamic polarization curves for mild steel in 0.5 M NaCl with 0–500 ppm concentration of apricot pomace extract.

LPR technique was used to investigate the time dependence of corrosion rate during immersion in inhibited and non-inhibited solutions. The corresponding dependences are given in Figure 5.

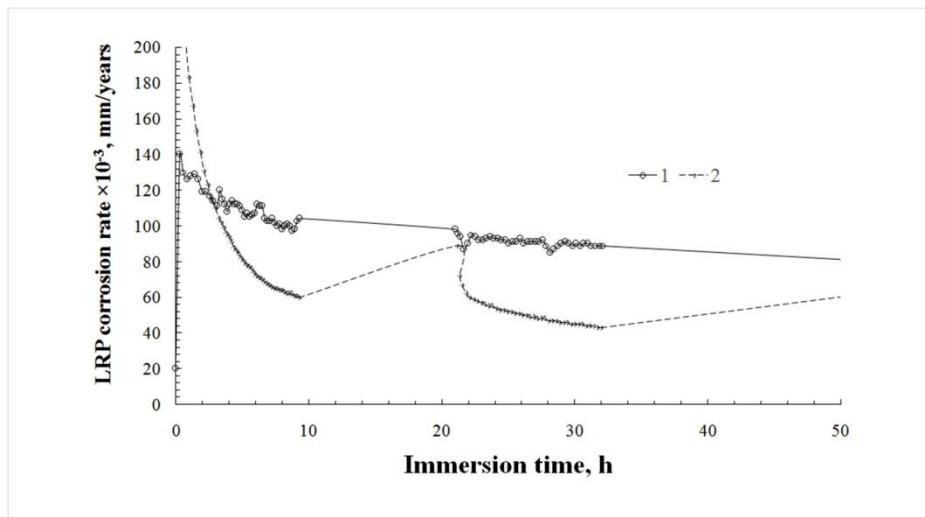


Figure 5. LPR corrosion rate of mild steel St3 in 0.5 M NaCl solution (1) and with apricot pomace extract (2).

Figure 5 depicts the corrosion rate (mm/year) for the electrode in 0.5 M NaCl saturated with inhibitor. Figure 5 shows that the values of corrosion rate are lower with the addition. The same behavior was shown in the case of the evolution of inhibition efficiency in function of immersion time (Figure 5). Such time dependence means that the formation of a barrier layer on the surface is a continuous process which requires at least 25–30 hours. The results obtained from weight loss and potentiodynamic polarization are in good agreement, and the compounds inhibition action could be proved by surface SEM and AFM images. It is well-known that FTIR spectroscopy is a powerful technique that can be used to determine the type of bonding of organic inhibitors absorbed on the metal surface (see Figure 6).

In the present study, FTIR spectra were used to support the fact that corrosion inhibition of mild steel in neutral media is due to the adsorption of inhibitor molecules on the mild steel surface and formation self-transformed the protective films. Fourier transform infrared spectroscopy was used to identify the functional groups and the structural units of the APE components. The FTIR spectroscopy of APE is shown in Figure 6. The bands at 2858 cm^{-1} and 1505 cm^{-1} are characteristic of C–H and C=C stretching vibrations, respectively. The bands below 920 cm^{-1} are characteristic of C–H bending vibrations. The presence of aliphatic CH_3 and CH_2 groups is indicated by absorption peaks at the $2930\text{--}2850\text{ cm}^{-1}$ (valence vibrations of CH_3 and CH_2 groups) and in the region of $1463\text{--}1377\text{ cm}^{-1}$ (deformation vibrations). The band at 1452 cm^{-1} can be attributed to C=C–C aromatic ring stretching. A number of peaks in the 950 cm^{-1} region indicate the vibrations of the CH bonds. There are also absorption bands in the range of $1611\text{--}1617\text{ cm}^{-1}$, 1505 and 3400 cm^{-1} , characteristic for vibrations of aromatic structures.

The peak centered at 1748 cm^{-1} is attributed to the stretching vibration of C=O. These observations clearly reveal that the APE is composed of many chemical compounds with hydroxyl, carboxylic and carbonyl functional groups, which may be involved in the mitigation of corrosion through coordination with iron atoms present on the mild steel surface. From the result of immersion, the metal in the solution and the corrosion inhibitor showed a stretch occurring in some organic functional groups. In Figure 6 (2), the FTIR spectrum of steel exposed in 0.5 M NaCl solution containing extract of apricot cake shows the stretching frequencies shifting to 1786 cm^{-1} , 1515 cm^{-1} , and 1711 cm^{-1} for C–H, C=C, and C=O vibrations, respectively. These band shifts confirm that the green inhibitor chemically and/or physically interacts with the metal surface [38, 39]. The intense band at 1752 cm^{-1} appeared is characteristic of ν (C=C) groups maybe corresponding to new groups of compounds (dimeric and trimeric polymer adducts) [10, 34]. This indicates the possible chemical change of the main compounds of APE once adsorbed on the mild steel surface and explains the highest protection values that achieved only in 48 h. Thus the anticorrosion properties of apricot cake extract cannot be explained only by the antioxidant properties of the molecules contained in these extract [41, 42].

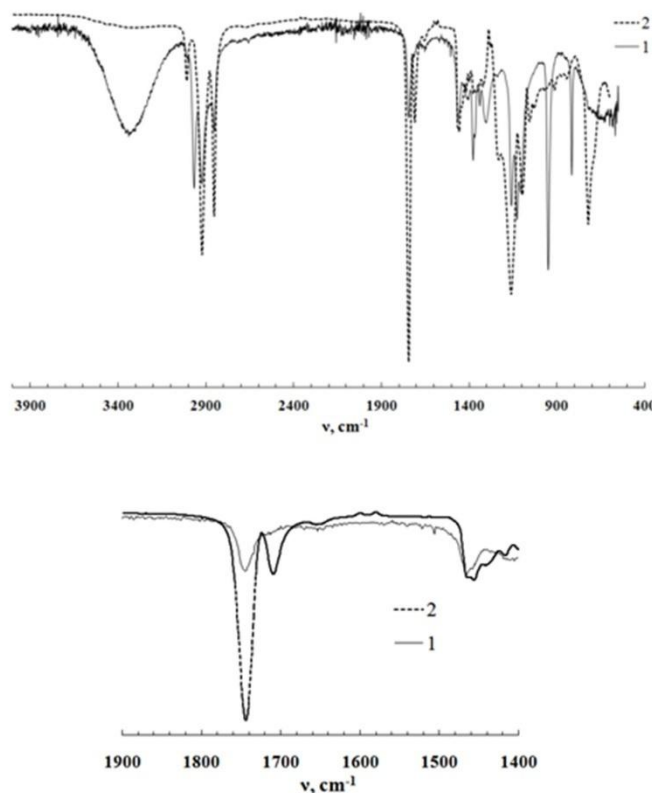


Figure 6. FTIR spectra of apricot pomace extract (1) and mild steel exposed in 0.5 M NaCl solution containing extract of apricot pomace (500 ppm; pre-treatment immersion time 48 h).

SEM analyses were conducted to characterize the protective layer that is formed on the mild steel surface. SEM micrographs (Figure 7b,c) of the steel surfaces in 0.5 M NaCl

solutions exhibit the changes which occurred during corrosion process in absence and presence of inhibitor.

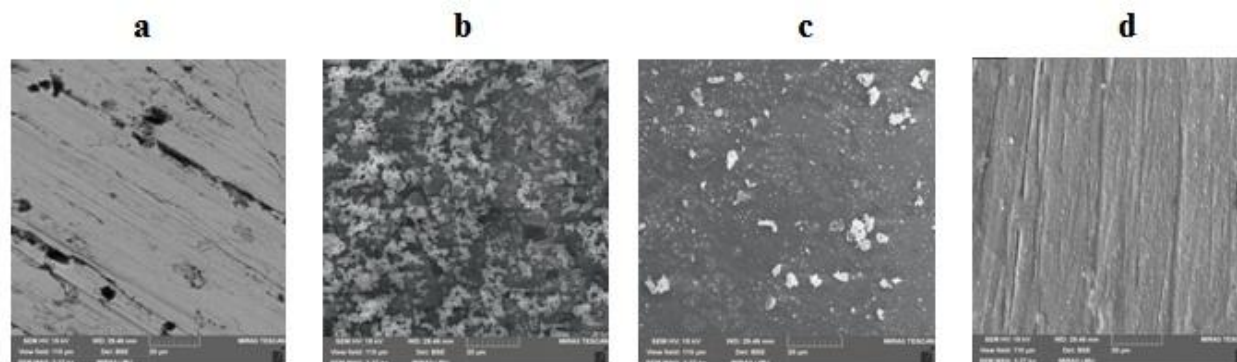


Figure 7. SEM micrographs (20 μm) of mild steel polished before immersion (a) and after 96 hours immersion time without inhibitor (b) in 0.5 M NaCl solution, after 48 (c) and 72 (d) hours immersion with 500 ppm of APE (d).

Close examination of the SEM images reveals that the specimens immersed in the inhibitor-containing solutions possess smoother surfaces compared with the specimens immersed in the blank 0.5 M NaCl solution, which have corroded, rough, coarse, and uneven surfaces. This observation indicated that the corrosion rate of mild steel was reduced in the presence of the plant extract, which might be due to the formation of a protective adsorbed film on the metal surface. Studies of the morphology of the film at a higher magnification (500 nm) indicate that the process of a protective layer formation is consistent, and has a layered structure. A similar structure of the film could be formed in the process of partial polymerization of pre-adsorbed compounds of the plant extract and layer-by-layer mechanism formation of a protective film. In addition to SEM, the corrosion samples were examined by AFM as well. The morphology of the film formed in the 0.5 M NaCl solution with 500 ppm of APE indirectly points on the possibility of polymer transformations of this inhibitor on the metal surface.

The surface morphologies of mild steel specimens under consideration were also investigated using AFM method in order to support the results of other experimental methods. The two-dimensional AFM image of steel before and after immersion in 0.5 M NaCl without and with 500 ppm of APE is shown in Figure 9.

The abraded mild steel surface is relatively smooth with distinct abrading scratches (Figure 9a,b). After the immersion in 0.5 M NaCl in the absence of inhibitor, however, the mild surface is highly damaged with deep holes and pits. AFM image analysis was implemented to get average roughness (see Table 5).

The slight roughness (4.6 nm) was observed on the polished steel surface. The average roughness value for the steel immersed in 0.5 M NaCl is 115.5 nm. This value suggests that steel immersed in solution of 0.5 M NaCl has a greater surface roughness than the polished metal surface. This indicates that the unprotected steel surface is rough,

due to the corrosion of steel in 0.5 M NaCl. In the presence of 500 ppm of ACP, the average roughness decreases to 56.7 nm, confirming the surface appears smoother. The smoothness of the surface is due to the formation of a protective film of APE surfactant on the Fe surface thereby inhibiting the corrosion of steel.

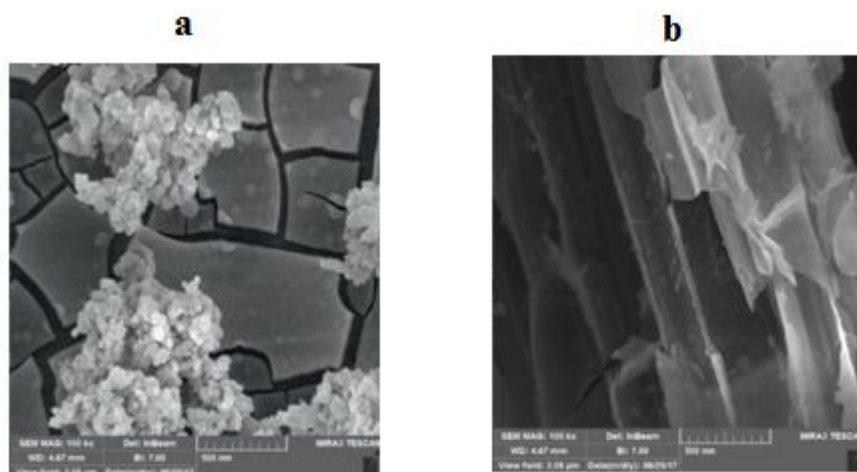


Figure 8. SEM micrographs (500 nm) of mild steel after 96 hours immersion time without inhibitor (a) in 0.5 M NaCl solution, after 72 (b) hours immersion with 500 ppm of APE.

Table 5. AFM data for steel surface immersed in inhibited and uninhibited APE solution in 0.5 M NaCl.

Sample	Average roughness (nm)
Polished steel (control)	4.6
Steel in 0.5 M NaCl (blank)	115.5
Blank + 550 ppm APE	56.7

Molecular structure and electronic characteristics are the key factors in establishing the adsorption ability of inhibitors on a metal surface [26–31]. Quantum chemical calculation was employed to gain insight into the inhibition mechanism of APE by examining the structure–reactivity correlation of the main compounds contained in APE. Figure 10 shows the frontier molecular orbital (FMO) density distributions, i.e., the HOMO and the LUMO. The calculated quantum chemical properties are summarized in Table 6.

From the frontier molecular orbital theory, it is known that transfer of electronic charge at the inhibitor/metal interface is dependent upon the highest occupied molecular orbital (HOMO) and lowest unoccupied molecular orbital (LUMO). The HOMO shows the inhibitor sites with the greatest ability of electron donation, while the inhibitor LUMO is indicative of its regions which accept electrons of the occupied orbitals of metal cations. Thus, a molecule with high-value E_{HOMO} (HOMO energy) and low-value E_{LUMO} (LUMO

energy) has the capacity to donate electrons to vacant orbital for electrophilic attack and accept electron for nucleophilic reaction, respectively.

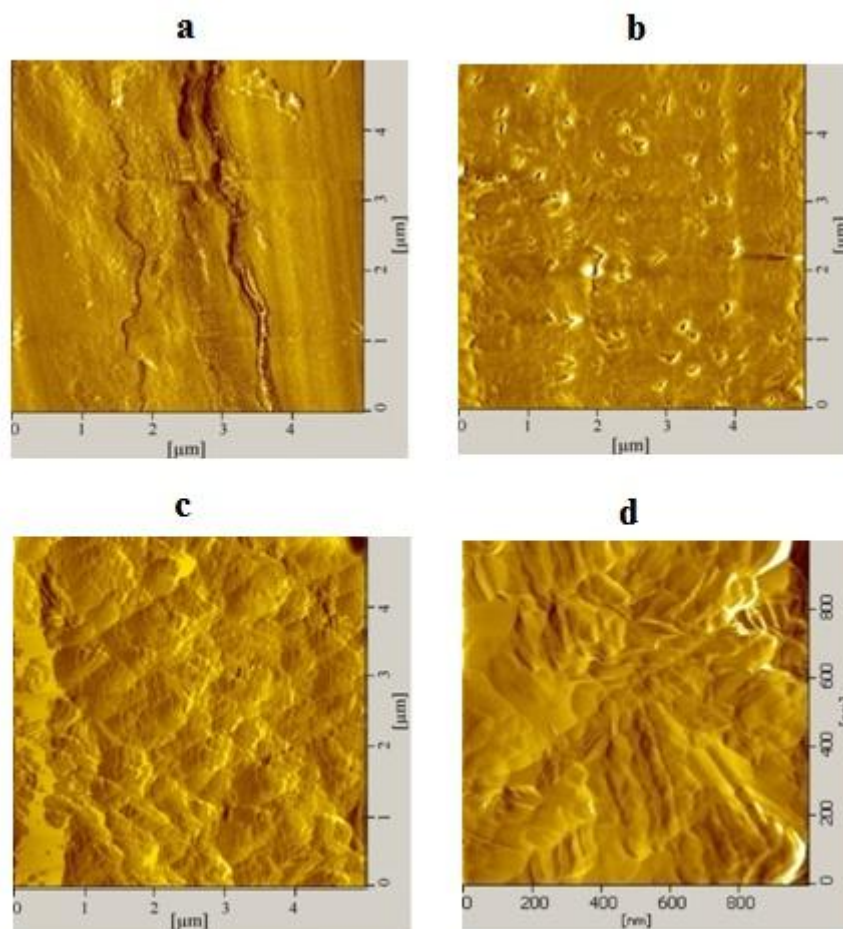


Figure 9. The two-dimensional AFM image of steel before (a) and after immersion in 0.5 M NaCl without (b) and with 500 ppm of APE (c, d).

The E_{HOMO} values for compounds increase in the following order: thymol < caffeic acid < catechin < linalool < gallic acid < 4-terpeniol < cyclocitral < benzaldehyde.

The analysis in Table 6 demonstrates that cyclocitral and benzaldehyde have near values of E_{HOMO} , which are the highest. This revealed their enhanced electron-donating ability. This suggests that a decreased energy gap of $\Delta E_{\text{H-L}}$ gives rise to an intensified charge sharing at the interface of inhibitor and metal, which in turn brings about strengthened interactions.

The calculated ΔE values of the compounds followed the order of caffeic acid < gallic acid < thymol < catechin < cyclocitral < benzaldehyde < linalool < 4-terpeniol, indicating that caffeic acid probably played the most prominent role in retarding the corrosion process.

To obtain a clear picture of the interaction between the molecules studied and mild steel surface, intermolecular parameters such as a charge transfer descriptors (ΔN) and the

associated energy change (ΔE) should be taken into account (see Table 7). The electronegativity (χ) is an indicator of the electron-attraction ability of a molecule. A higher χ corresponds to a lower chance of electron donation from the molecule and *vice versa* [26–31]. This means higher electronegativity values correspond to higher inhibition efficiencies. According to Table 6, the electronegativity value of the compound increases in order thymol > catechin > caffeic acid > gallic acid > linalool > 4-terpeniol > cyclocitral > benzaldehyde.

All the investigated molecules had electronegativity values lower than Fe electronegativity (7 eV mol^{-1}).

Hence, the studied molecules are expected to offer electrons to Fe. Moreover, a higher value of global hardness (η) indicates a higher resistance of a molecule toward charge transfer [26–31, 41–44]. The calculations indicate that caffeic acid has the lowest value, which means the highest reactivity among the other inhibitor and accordingly the highest inhibition efficiency.

Global electrophilicity index (ω) informs about the nucleophilic or electrophilic character of the molecule. The higher the value of electrophilicity index, the best the capacity of the molecule to accept electrons. Benzaldehyde has the greatest electrophilicity value (2.30659 eV/mol), which reflects its nucleophilicity, *i.e.* its good ability to donate electrons.

Table 6. Calculated quantum chemical properties for the most stable conformations of the major components of the cake apricot extracts.

Compounds	E_{HOMO}	E_{LUMO}	HOMO–LUMO gap (ΔE)
Benzaldehyde	–10.2236	–0.5566	9.6669
Linalool	–9.5938	0.8384	10.4322
Gallic acid	–9.61154	–0.7838	8.8277
Thymol	–8.83529	0.0601	8.8954
Cyclocitral	–10.1740	–0.5268	9.6472
Caffeic acid	–9.1764	–1.11589	8.0605
4–Terpeniol	–9.8119	0.68560	10.4975
Catechin	–9.2143	–0.1269	9.0874

According to Lukovits, if electron fraction transferred (ΔN) < 3.6, the chemisorption and inhibition efficiency tendency increases with the increase in the electron-donating ability at the metal surface.

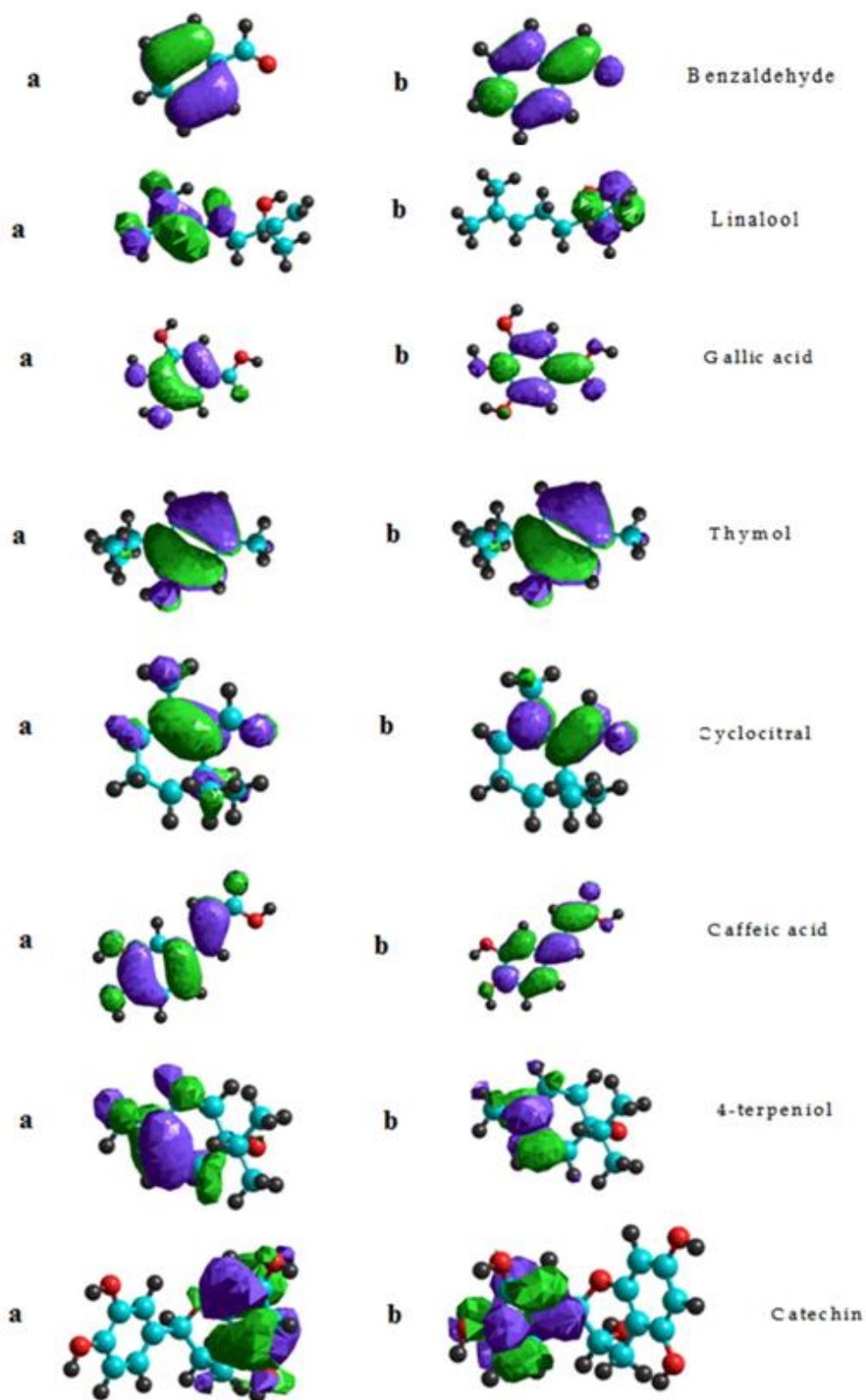


Figure 10. The frontier molecule orbital density distributions of studied compounds; highest occupied molecular orbital (E_{HOMO}) (a) and the lowest unoccupied molecular orbital (E_{LUMO}) (b).

Table 7. Calculated quantum chemical properties for the most stable conformations of the major components of the APE.

Compounds	Electronegativity, χ	Hardness, η	Electrophilicity index, ω	ΔN	ΔE
Benzaldehyde	5.3901	4.8334	1.3475	0.166	0.0168
Linalool	5.2161	4.3777	1.3040	0.203	0.0090
Gallic acid	5.1976	4.4138	1.2994	0.204	0.0081
Thymol	4.3875	4.4476	1.0969	0.293	0.0105
Cyclocitral	5.3504	4.8236	1.3376	0.171	0.0146
Caffeic acid	5.1461	4.0302	1.2865	0.230	0.0066
4-Terpeniol	5.2487	4.5631	1.3122	0.191	0.0101
Catechin	4.6706	4.5436	1.1677	0.256	0.0012

All the extract components possess ΔN values lower than 3.6. This suggested their great tendency to interact with the metal surface. This shows that as the strength of the iron inhibitor bond increases (as a result of increasing ΔN), the degree of corrosion inhibition due to chemisorption is increased.

As expected, the most abundant compounds identified in the sample of apricot cake extract contained oxygen atoms with lone electron pairs and aromatic rings with delocalized electrons, which enabled them to adsorb on the metallic surface forming protective layers, which retarded the corrosion process.

Corrosion inhibition explanation

The presence of such numerous organic compounds makes it rather difficult to attempt to assign the observed corrosion behavior to a particular constituent, but still a possible interpretation of our results may be traced out. The apricot cake extract contains various bioactive molecules, such as flavonoids (10.04 percent) aldehydes (18 percent), terpene alcohols, and acids (18.91 percent). The investigated extract of apricot cake has a high antioxidant activity, which is an indirect evidence of its potentially high anti-corrosion properties. The anticorrosion properties of apricot cake extract, cannot be explained only by the antioxidant properties of the polyphenol molecules, as flavonoids (catechin, quercetin), contained in this extract. In presence of extract, the corrosion rate is actually reduced by the progressive formation of a covering film. This film could be formed by the compounds with unknown antioxidant properties extracted from the apricot cake, but which could be transformed (polymerized) on the steel surface/in solution and cover the steel surface by the film with higher protective properties. In the early stage of immersion (1–20 hours), the formation of a protective layer occurred according to the mechanism of physical adsorption and to the precipitation of more adsorption active compounds. This layer acts a self-protective barrier, characterized low degree of the protective. However at

increase the time of film forming to 30–50 hours, the primary protective layer is transformed (polymerized) and other higher molecular weight components of the extract to exhibit the protective effect. A new self-transformed protective layer possesses more high protective properties. In this way, the high inhibitory efficacy of apricot cake extract on steel in neutral solution is the consequence of the formation of the protective film from the main compounds of extract and the products of their chemical transformations on the corroding surface.

Conclusions

Combining experiments and theoretical calculations, APE has the potential to be developed as an environmentally friendly inhibitor for mild steel corrosion. Characteristics of APE are nontoxic, inexpensive, readily available, and easily extracted. The potentiodynamic polarization studies indicated that APE acts as a mixed-type inhibitor. Weight loss measurements proved a highly protective effect obtained in the presence of APE after several hours of immersion which remains stable over the time. In the investigated experimental condition, the maximum inhibiting efficiency in the range of 94.6% was obtained by the addition of 500 ppm APE, after about 48 h of exposure to the inhibitor-containing electrolyte. The results of the surface analysis performed by SEM and AFM confirm that APE is able to retard the steel corrosion by the formation of a compact and homogeneous surface layer on the metallic surface. Although GC-MS analysis identified the most abundant compounds present in the APE, due to its complex chemical composition, it is difficult to assign the inhibitive effectiveness to a specific constituent. Further studies will focus on the study of the antioxidant and inhibitory properties of the main components of the plant extract, as well as studying the correlation between these two parameters. The results obtained will make it possible to confirm or disprove the importance of the antioxidant properties of the extract, as one of the parameters of the predictive assessment of the inhibitory ability of plant extracts when used as a means of corrosion protection.

References

1. O.K. Abiola, N.C. Oforka, E.E. Ebenso and N.M. Nwinuka, *Anti-Corros. Methods Mater.*, 2007, **54**, no. 4, 219–224. doi: [10.1108/00035590710762357](https://doi.org/10.1108/00035590710762357)
2. Yu.I. Kuznetsov, *Int. J. Corros. Scale Inhib.*, 2015, **4**, no. 4, 284–310. doi: [10.17675/2305-6894-2015-4-4-1](https://doi.org/10.17675/2305-6894-2015-4-4-1)
3. G. Vasyliiev, A. Brovchenko, and Y. Herasymenko, *Chem. Chem. Technol.*, 2013, **7**, no. 4, 477–482.
4. Yu.I. Kuznetsov, *Int. J. Corros. Scale Inhib.*, 2016, **5**, no. 4, 282–318. doi: [10.17675/2305-6894-2016-5-4-1](https://doi.org/10.17675/2305-6894-2016-5-4-1)
5. Yu.I. Kuznetsov, *Int. J. Corros. Scale Inhib.*, 2017, **6**, no. 4, 209–239. doi: [10.17675/2305-6894-2017-6-3-1](https://doi.org/10.17675/2305-6894-2017-6-3-1)

6. Yu.I. Kuznetsov, *Int. J. Corros. Scale Inhib.*, 2017, **6**, no. 4, 384–327. doi: [10.17675/2305-6894-2017-6-4-3](https://doi.org/10.17675/2305-6894-2017-6-4-3)
7. P.B. Raja and M.G. Sethuraman, *Mater. Lett.*, 2008, **62**, no. 1, 113–116. doi: [10.1016/j.matlet.2007.04.079](https://doi.org/10.1016/j.matlet.2007.04.079)
8. K. Nasr, M. Fedel, K. Essalah, F. Deflorian and N. Souissi, *Anti-Corros. Methods Mater.*, 2018, **65**, no. 3, 292–309. doi: [10.1108/ACMM-12-2017-1869](https://doi.org/10.1108/ACMM-12-2017-1869)
9. S. Javadiana, B. Darbasizadeh, A. Yousefi, F. Ektefa, N. Dalir and J. Kakemam, *J. Taiwan Inst. Chem. Eng.*, 2017, **71**, 344–354. doi: [10.1016/j.jtice.2016.11.014](https://doi.org/10.1016/j.jtice.2016.11.014)
10. G. Vasylyev and V. Vorobiova, *Mater. Today: Proc.*, 2019, **6**, no. 2, 178–186. doi: [10.1016/j.matpr.2018.10.092](https://doi.org/10.1016/j.matpr.2018.10.092)
11. N. Bhardwaj, D. Prasad and R. Haldhar, *J. Bio- Tribo-Corros.*, 2018, **4**, no. 4, 61. doi: [10.1007/s40735-018-0178-4](https://doi.org/10.1007/s40735-018-0178-4)
12. T.K. Bhuvanewari, V.S. Vasantha and C. Jeyaprabha, *Silicon*, 2018, **10**, no. 5, 1793–1807. doi: [10.1007/s12633-017-9673-3](https://doi.org/10.1007/s12633-017-9673-3)
13. A.S. Yaro, A.A. Khadom and R.K. Wael, *Alexandria Eng. J.*, 2013, **52**, no. 1, 129–135. doi: [10.1016/j.aej.2012.11.001](https://doi.org/10.1016/j.aej.2012.11.001)
14. A. Saxena, D. Prasad and R. Haldhar, *Bioelectrochemistry*, **124**, 156–164. doi: [10.1016/j.bioelechem.2018.07.006](https://doi.org/10.1016/j.bioelechem.2018.07.006)
15. S. Javadian, A. Yousefi and J. Neshati, *Appl. Surf. Sci.*, 2013, **285**, 674–681. doi: [10.1016/j.apsusc.2013.08.109](https://doi.org/10.1016/j.apsusc.2013.08.109)
16. J. Gopal, A. Shadma, S. Shanthi and P. Rajiv, *Corros. Sci.*, 2015, **90**, 107–117. doi: [10.1016/j.corsci.2014.10.002](https://doi.org/10.1016/j.corsci.2014.10.002)
17. V.I. Vorobyova, M.I. Skiba, A.S. Shakun and S.V. Nahirniak, *Int. J. Corros. Scale Inhib.*, 2019, **8**, no. 2, 150–178. doi: [10.17675/2305-6894-2019-8-2-1](https://doi.org/10.17675/2305-6894-2019-8-2-1)
18. V. Oreopoulou and C. Tzia, *Antioxidants, and Colorants*, 2007, Springer, Boston, MA. doi: [10.1007/978-0-387-35766-9_11](https://doi.org/10.1007/978-0-387-35766-9_11)
19. L.G. Johnsen, P.B. Skou, B. Khakimov and R. Bro, *J. Chromatogr. A*, 2017, **1503**, 57–64. doi: [10.1016/j.chroma.2017.04.052](https://doi.org/10.1016/j.chroma.2017.04.052)
20. S.E. Stein, *J. Am. Soc. Mass Spectrom.*, 1999, **10**, no. 8, 770–781. doi: [10.1016/S1044-0305\(99\)00047-1](https://doi.org/10.1016/S1044-0305(99)00047-1)
21. P.M. Pilar and M.A. Pineda, *Anal. Biochem.*, 1999, **269**, no. 2, 337–341. doi: [10.1006/abio.1999.4019](https://doi.org/10.1006/abio.1999.4019)
22. I. Horcas, R. Fernandez, J.M. Gomez-Rodriguez, J. Colchero, J. Gomez-Herrero and A.M. Baro, *Rev. Sci. Instrum.*, 2007, **78**, 013705. doi: [10.1063/1.2432410](https://doi.org/10.1063/1.2432410)
23. Standard practice for laboratory immersion corrosion testing of metals, G 31–72.
24. H.S. Vasylyev, *Mater. Sci.*, 2013, **48**, no. 5, 694–696. doi: [10.1007/s11003-013-9556-8](https://doi.org/10.1007/s11003-013-9556-8)
25. Y.S. Herasymenko and H.S. Vasylyev, *Mater. Sci.*, 2009, **45**, no. 5, 899–904. doi: [10.1007/s11003-010-9256-6](https://doi.org/10.1007/s11003-010-9256-6)
26. S.K. Saha, P. Ghosh, A. Hens, N.C. Murmu and P. Banerjee, *Phys. E (Amsterdam, Neth.)*, 2015, **66**, 332–341. doi: [10.1016/j.physe.2014.10.035](https://doi.org/10.1016/j.physe.2014.10.035)

27. V. Vorobyova, O. Chygyrynets', M. Skiba, I. Trus and S. Frolenkova, *Chem. Chem. Technol.*, 2018, **12**, no. 3, 410–418. doi: [10.23939/chcht12.03.410](https://doi.org/10.23939/chcht12.03.410)
28. V. Vorobyova, O. Chygyrynets, M. Skiba, *J. Chem. Technol. Metall.*, 2018, **53**, no. 2, 336–345. https://dl.uctm.edu/journal/node/j2018-2/22_17_91_p_336_345.pdf
29. P. Durainatarajan, M. Prabakaran, S. Ramesha and V. Periasamy, *Mater. Today: Proc.*, 2018, **5**, no. 8, 16226–16236. doi: [10.1016/j.matpr.2018.05.114](https://doi.org/10.1016/j.matpr.2018.05.114)
30. F. Bentiss, B. Mernari, M. Traisnel, H. Vezin and M. Lagrenée, *Corros. Sci.*, 2011, **53**, 487–495. doi: [10.1016/j.corsci.2010.09.063](https://doi.org/10.1016/j.corsci.2010.09.063)
31. S.N. Victoria, R. Prasad and R. Manivannan, *Int. J. Electrochem. Sci.*, 2015, **10**, 2220–2238. <http://www.electrochemsci.org/papers/vol10/100302220.pdf>
32. S.E. Stein, *J. Am. Soc. Mass Spectrom.*, 1999, **5**, no. 10, 770.
33. V. Vorobyova, O. Chygyrynets', M. Skiba and I. Kurmakova, *Int. J. Corros. Scale Inhib.*, 2017, **6**, no. 4, 485–503. doi: [10.17675/2305-6894-2017-6-4-8](https://doi.org/10.17675/2305-6894-2017-6-4-8)
34. V. Vorobyova, O. Chygyrynets', T. Overchenko and M. Skiba, *Chem. Chem. Technol.*, 2019, **13**, no. 2, 261–268. doi: [10.23939/chcht13.02.261](https://doi.org/10.23939/chcht13.02.261)
35. V. Vorobyova, M. Skiba and O. Chygyrynets', *Pigm. Resin Technol.*, 2019, **48**, no. 2, 137–147. doi: [10.1108/PRT-03-2018-0025](https://doi.org/10.1108/PRT-03-2018-0025)
36. O.E. Chyhyrynets' and V.I. Vorob'iova, *Mater. Sci.*, 2013, **49**, 318–325. doi: [10.1007/s11003-013-9617-z](https://doi.org/10.1007/s11003-013-9617-z)
37. O.E. Chyhyrynets, Y.F. Fateev, V.I. Vorobiova and M.I. Skyba, *Mater. Sci.*, 2016, **51**, 644–651. doi: [10.1007/s11003-016-9886-4](https://doi.org/10.1007/s11003-016-9886-4)
38. V. Vorobyova, O. Chygyrynets', M. Skiba, T. Zhuk, I. Kurmakova and O. Bondar, *Int. J. Corros. Scale Inhib.*, 2018, **7**, no. 2, 185–202. doi: [10.17675/2305-6894-2018-7-2-6](https://doi.org/10.17675/2305-6894-2018-7-2-6)
39. V. Vorobyova, O. Chygyrynets', M. Skiba, I. Trus and S. Frolenkova, *Chem. Chem. Technol.*, 2018, **12**, no. 3, 410–418. doi: [10.23939/chcht12.03.410](https://doi.org/10.23939/chcht12.03.410)
40. O.E. Chyhyrynets' and V.I. Vorob'iova, *Mater. Sci.*, 2013, **49**, 318–325. doi: [10.1007/s11003-013-9617-z](https://doi.org/10.1007/s11003-013-9617-z)
41. K. Fredy and A.M. Kartika, *Prog. Org. Coat.*, 2015, **88**, 256–262. doi: [10.1016/j.porgcoat.2015.07.010](https://doi.org/10.1016/j.porgcoat.2015.07.010)
42. X.H. Li, S.D. Deng, X.G. Xie and H. Fu, *Corros. Sci.*, 2014, **87**, 15–26. doi: [10.1016/j.corsci.2014.05.013](https://doi.org/10.1016/j.corsci.2014.05.013)
43. A. Singh, V.K. Singh and M.A. Quraishi, *Int. J. Corros.*, 2010, 1–10. doi: [10.1155/2010/275983](https://doi.org/10.1155/2010/275983)
44. L. Li, X. Zhang, J. Lei, J. He, S. Zhang, F. Pan, *Corros. Sci.*, 2012, **63**, 82–90. doi: [10.1016/j.corsci.2012.05.026](https://doi.org/10.1016/j.corsci.2012.05.026)

